How Does Moisture Affect the Physical Property of Memristance for Anionic–Electronic Resistive Switching Memories?

*Felix Messerschmitt, Markus Kubicek, and Jennifer L. M. Rupp**

Memristors based on anionic–electronic resistive switches represent a promising alternative to transistor-based memories because of their scalability and low power consumption. To date, studies on resistive switching have focused on oxygen anionic or electronic defects leaving protonic charge-carrier contributions out of the picture despite the fact that many resistive switching oxides are well-established materials in resistive humidity sensors. Here, the way memristance is affected by moisture for the model material strontium titanate is studied. First, characterize own-processed Pt|$SrTiO_{3-\delta}$|Pt bits via cyclic voltammetry under ambient conditions are thoroughly characterized. Based on the high stability of a non-volatile device structures the impact of relative humidity to the current–voltage profiles is then investigated. It is found that Pt|$SrTiO_{3-\delta}$|Pt strongly modifies the resistance states by up to 4 orders of magnitude as well as the device's current–voltage profile shape, number of crossings, and switching capability with the level of moisture exposure. Furthermore, a reversible transition from classic memristive behavior at ambient humidity to a capacitively dominated one in dry atmosphere for which the resistive switching completely vanishes is demonstrated for the first time. The results are discussed in relation to the changed Schottky barrier by adsorbed surface water molecules and its interplay with the charge transfer in the oxide.

1. Introduction

Memory technologies based on electronically operated transistors, for instance, dynamic random-access memory (DRAM) and flash memory, are currently reaching their physical limits in scalability.[1] Driven by the growing demands on fast-data transfer, increased computational speed and memory density, the development of novel material structures and operation concepts is one of the major challenges of the 21st century. Here, memristors deployed as resistive-RAM (ReRAM) represent a promising alternative to replace state-of-the-art transistor-based memories in the near future.[1] In these ReRAMs, ionic carriers are moved under high electric fields besides their electronic counterparts, resulting in superior memory storage with fast ns-read/write speeds, low energy consumption, and high retention.[2] The potential of these ionically controlled resistive switches is amplified by their multiple accessible resistance states even going beyond binary logics.[2] Although the first demonstration of rapid resistance changes in oxides upon bias pulses dates back to the 1960s,[3] it was not until 2008 that Strukov and co-workers[4] connected the experimental results of their fabricated Pt|TiO_2|Pt resistive switches to the memristor theory by Chua.[5] Today it is generally accepted that simple metal|oxide|metal structures can show memristive behavior[4,5] under high local electric field strengths (>10^6 Vm^{-1}) [2,6] and different resistive states can be addressed via the current flux history. Mainly two types of oxide-based ReRAMs exist, namely cationic and anionic resistive switches, differing in their type of main ionic-carrier contribution accountable for the memristance.[6] In anionic–electronic resistive switches the migration of oxygen anions via defects (oxygen vacancies), which is facilitated under high electrical fields, is responsible for the controlled resistance changes. These resistive switches operate via local valence changes of the transition metal oxide which is balanced by electronic carriers. The electric conductivity, σ_{total}, for an anionic–electronic resistive switching oxide can be described using the Kröger–Vink notation:

$$\sigma_{total} = q\eta_{h^\bullet} c_{h^\bullet} + q\eta_{e'} c_{e'} + 2q\eta_{V_O^{\bullet\bullet}} c_{V_O^{\bullet\bullet}} \quad (1)$$

where q denotes the elementary charge, η_j the mobility and c_j the concentration, of the single charge carrier species, j. $h^\bullet$ are the holes, e' the electrons and $V_O^{\bullet\bullet}$ the oxygen vacancies. Material examples include $SrTiO_3$, $SrZrO_3$, ZrO_2, TiO_2, SiO_2, $HfO_{2-\delta}$, SnO_2, $Ta_2O_{5-\delta}$, $BaTiO_3$, $(La,Sr)MnO_3$, $(Pr,Ca)MnO_3$, $(La,Sr)(Co,Fe)O_3$, and $CaCu_3Ti_4O_{12}$ with metallic or oxide electrodes such as Pt, Au, Ni, Pd, Nb:$SrTiO_3$, or $SrRuO_3$.[2,6–9]

In this study, we work with strontium titanate, $SrTiO_{3-\delta}$, as the resistive switching oxide which is a well-suited model material to investigate the role of defects and charge carriers

F. Messerschmitt, Dr. M. Kubicek, Prof. J. L. M. Rupp
Electrochemical Materials
Department of Materials, ETH Zurich
Hönggerbergring 64, 8093 Zurich, Switzerland
E-mail: jennifer.rupp@mat.ethz.ch

DOI: 10.1002/adfm.201501517

on the resistive switching phenomena because of the following reasons:

- $SrTiO_{3-\delta}$ shows promising non-volatile oxygen anionic-type controlled resistive switching at electric field strengths of more than 10^6 V m^{-1} with R_{off}/R_{on} ratios of up to 100, a retention of 10^5 s, and an endurance of 10^6 cycles.[10–18] Recently, we have reported on the successful distinction of capacitive and memristive contributions to the resistive switching and a facilitated oxygen migration for memristive conditions with diffusion constants of up to 3×10^{-15} m^2 s^{-1} at electric field strengths of 6.2×10^6 V m^{-1} for Pt|$SrTiO_{3-\delta}$|Pt bits.[18]
- The oxide has a single-phase cubic perovskite structure that is stable over a large temperature range of 105–1913 K,[19] and has a large stability range of oxygen non-stoichiometry down to $SrTiO_{2.5}$.[20]
- The defect chemistry, especially at high temperatures, is well established and the mixed oxygen anionic–electronic conduction mechanism is well understood.[21] Under ambient conditions it is a predominant p-type conductor with an electrolytic domain boundary at lower oxygen partial pressures of roughly 10^{-3} atm.[22] Very recently, reports have appeared on the changes in the local dislocation concentrations that alter the oxygen diffusion coefficients under high fields during switching. These changes and their direct implication on the electronic carrier diffusion have been discussed in theory[23,24] and are supported by transient-transport experiments for $SrTiO_{3-\delta}$.[18]

Although many reports have been published on the resistive switching of $SrTiO_3$, the detailed resistive switching mechanism remains under debate.[13,25,26] To date, fundamental resistive switching studies on $SrTiO_3$ have focused primarily on the anion contribution, namely the defects in the anionic sublattice as oxygen vacancies, $V_O^{\cdot\cdot}$, and the location of these defects in the resistive switches.[6,11,27] For example, the role of the Schottky barrier at the metal|oxide interfaces was highlighted by Sawa,[26] whereas for instance Waser and co-workers[13] emphasized that the formation and rupture of conductive filaments is responsible for the resistive switching. Typical analyzing methods to characterize the resistive switching involve cyclic voltammetry,[6] conducting atomic force microscopy,[25,28,29] chronoamperometry,[18,30] impedance spectroscopy,[28] oxygen tracer diffusion,[23] and electro-coloration experiments.[31] As such, these experiments predominantly address the role of the main charge carriers (electrons and oxygen anions) on the several orders of magnitude switchable resistance states. However, many of these experiments do not allow the direct determination of the predominant charge-carrier type when there are two- or even more charge-carrier types involved. This also leaves out the contribution of protonic charge-carrier species or interactions with hydroxyl groups created by ambient moisture exposure. Even for $SrTiO_3$, one of the most investigated materials in anionic–electronic resistive switching, it remains unknown whether moisture can affect resistive switching and the physical property of memristance.

Interestingly, numerous oxides currently used as resistive switching oxides are known to show variations in their resistance upon moisture exposure at low electric field strengths. Examples include the tunable ohmic resistance states upon humidity exposure of the oxides $SrTiO_3$,[32] CeO_2,[33,34] TiO_2,[32] $BaTiO_3$,[32] SnO_2,[35] and Y_2O_3:ZrO_2.[36] In these materials, the capability of incorporating hydroxyl ions (i.e., OH intermediates) into these oxide surfaces and into the bulk by interaction with oxygen vacancies have formed the technological base for today's ceramic humidity sensors.[32,37–39]

The reaction of oxygen-deficient $SrTiO_{3-\delta}$ with moisture has been revealed to include clear interactions with the anionic, electronic, and protonic carriers.[34,40–43] Water molecules from the gas phase are first adsorbed at the surface and can subsequently be incorporated into the bulk oxide phase via the following hydration reaction:[21,40,41]

$$H_2O + O_o^x + V_o^{\cdot\cdot} \rightleftharpoons 2OH_o^{\cdot} \quad (2)$$

Taking the protonic contribution into account the total conductivity of the switching oxide, see Equation (1), has to be extended to:

$$\sigma_{total} = q\eta_{h^{\cdot}}c_{h^{\cdot}} + q\eta_{e'}c_{e'} + 2q\eta_{V_o^{\cdot\cdot}}c_{V_o^{\cdot\cdot}} + q\eta_{OH_o^{\cdot}}c_{OH_o^{\cdot}} \quad (3)$$

where $OH_{\dot{O}}$ indicates a proton bound to oxygen in the metal oxide. At elevated water concentration the surface, interface, and grain-boundary proton conduction mechanisms in the oxides become more relevant for conductivity changes rather than pure bulk protonic conduction.[38,42] This means that water interacts with the metal oxide resulting in a first layer being chemically adsorbed as hydroxyl groups, whereby subsequent water layers may become physically adsorbed to the oxide's lattice. In this state, protonic defects can diffuse over the hydroxyl groups, cascading as additional protonic conductivity via the "Grotthuss mechanism" in addition to the oxygen anionic and electronic contributions.[42–47] It is important to note, however, that conductivity changes by moisture depend strongly on the temperature and porosity of the metal oxide,[32,38] and it can also be influenced by reactions of other ambient gases at the interface, for instance reactions with CO or CO_2.[32] Additionally to the conductivity changes due to moisture, a possible water-splitting reaction could interfere with the memristance activated through the extreme conditions prevailing in resistive switching devices, namely the high electrical field strength. Although the active modulation principles of ohmic resistances and surface potentials of oxides used in ceramic humidity sensors have been evidenced before, the effect of moisture and the interaction of hydroxyl groups with oxygen vacancies and electrons on the physical property of memristance for anionic–electronic resistive switches has thus far not been elucidated.

This is in contrast with recent advances in the field of cationic–electronic resistive switches: first reports from Waser et al.[48,49] have shown that the injection of copper cations from the electrode into the oxide and the resulting formation of metallic filaments, for instance Cu-filaments in a Cu|SiO_2|Pt resistive switch, proceeds in parallel with the reduction of moisture acting as a counter/charge reaction at the platinum electrode. Additionally, Tsuruoka et al.[43] have reported, among others, that a hydrogen-bond network formed by moisture adsorption facilitates the Cu ionic migration along the grain boundaries of the oxide, a conclusion that could be drawn from

comparing Cu|SiO_2|Pt and Cu|Ta_2O_3|Pt cationic–electronic devices. Here, the SET and RESET voltages were significantly altered by the relative humidity for the cationic–electronic resistive switches.

From a fundamental perspective it is exciting to uncover if and how the basic property of memristance is affected by moisture and protons as additional carrier species interacting with oxygen anions and electrons for anionic–electronic resistive switches. For decades the ohmic resistance and interface resistive modulations of mixed conducting oxides have been researched with respect to humidity exposure. In this work we turn our focus on memristive anionic–electronic switches and investigate the interplay of oxygen anionic, electronic, and protonic charge carriers and fluxes for the constituents of the oxide material. These can play a key role in understanding how defects on the atomic level can interact with the surfaces and bulk of the oxide compound and whether adsorbing ambient species can contribute to the property of memristance in oxide-based switches. Therefore, we need to carefully examine how this may affect future material selection and engineering strategies for enhanced performing ReRAMs.

In this work, we investigate and demonstrate the controlled modulation of memristance upon humidity exposure in strontium titanate-based switches. For this, we have fabricated model 2-terminal Pt|$SrTiO_{3-\delta}$|Pt resistive switching bits with cross-bar array structures and single micro-electrodes. By adopting the relative humidity level during stable operation of the model switches in cyclic voltammetry experiments we were able to probe for the first time an oxide model system with oxygen vacancies and electronic carriers and the direct implication of moisture on the non-equilibrium states of the resistive switch. The current–voltage (I–V) profiles, their low to high resistance state ratio, switching capability, and overall conduction changes are investigated relative to the moisture and electric field strength variations. Hence, the experimental approach gives first insights to the fundamental question whether the memristance of anionic–electronic resistive switches, exemplified by $SrTiO_{3-\delta}$, is affected by atmospheric changes and whether this can actively be used. The implications this has for the redox-kinetics and carriers involved is also discussed in view of future device operation and integration of $SrTiO_3$-based anionic–electronic ReRAMs.

2. Results and Discussion

2.1. Resistive Switching Performance under Ambient Conditions

We studied the resistive switching based on oxygen anionic–electronic transfer with our own-fabricated bit structures in cross-plane configuration consisting of two platinum electrodes separated by a $SrTiO_{3-\delta}$ thin film, see **Figure 1**a. Several micro-electrodes were structured onto the sample to characterize the memristive behavior and assure reproducibility of the resistive switching measurements including a close-to-application multi-bit cross-bar array, see Figure 1b. The scanning electron microscopy image of the cross-section of a single bit is shown in Figure 1c. It reveals a good adhesion between the Pt electrodes and the oxide film and also a crack-free and dense $SrTiO_{3-\delta}$ film microstructure of 760 nm in thickness. The $SrTiO_{3-\delta}$ film

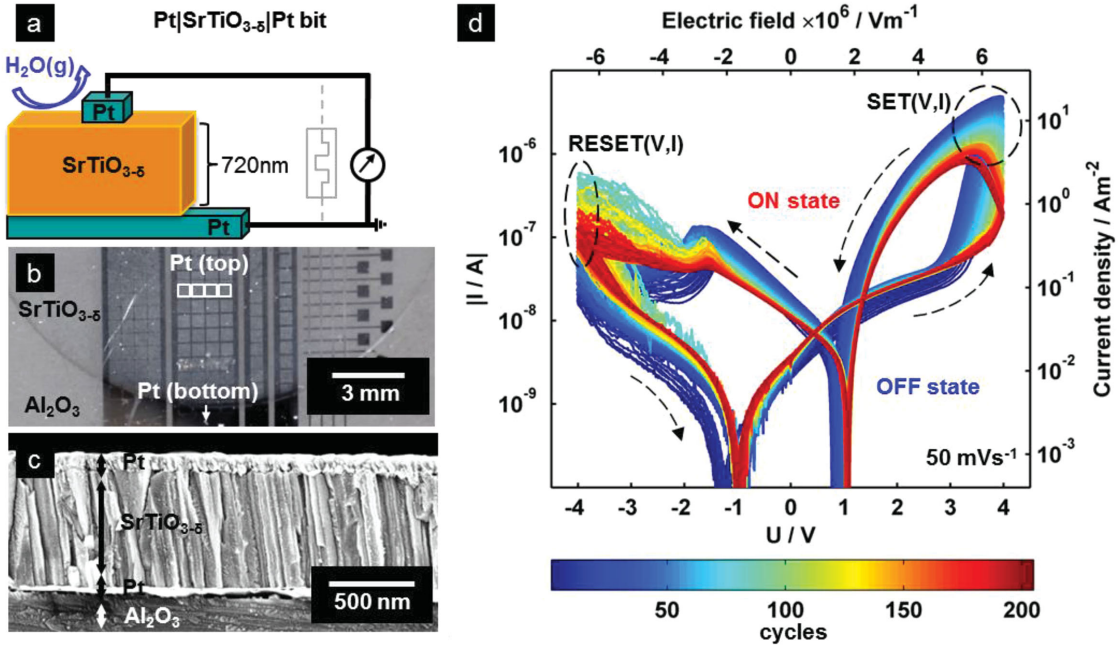

Figure 1. a) Schematic representation of a single Pt|$SrTiO_{3-\delta}$|Pt memristive bit exposed to humidified air with its corresponding circuit symbol. b) Photograph of the measured sample showing several electrodes for cross-plane electrical measurements including a multi-bit crossbar array. c) Scanning electron microscopy image of a cross section of the thin film showing the polycrystalline columnar growth during pulsed laser deposition. d) Results of cyclic voltammetry measurements of 200 consecutive cycles at a constant sweep rate of 50 mV s^{-1} showing a very stable and robust resistive switching behavior.

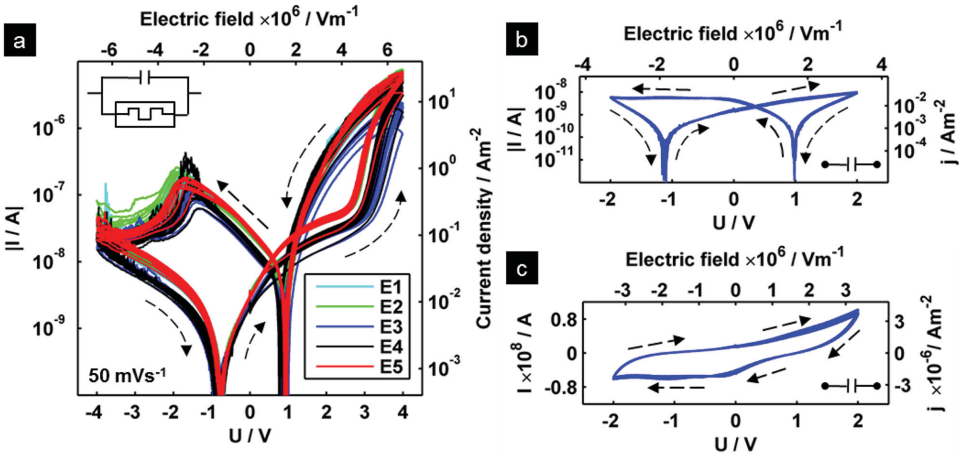

Figure 2. Uniformity of the device and capacitive contributions: a) Cyclic voltammetry measurements on five different microelectrode sets, *E1* to *E5*, between ±4V showing uniformity and no differences in switching between the single electrodes. b,c) Cyclic voltammetry measurements for a bias of ±2 V in log and linear scale, respectively.

exhibits a typical polycrystalline and columnar microstructure typical for pulsed laser deposition thin-film growth.[50–52] The cubic perovskite phase of the thin film was confirmed by X-ray diffraction measurements in accordance to previously published results,[53] see Figure S1 in the Supporting Information. In a first step, we detailed the resistive switching characteristics using cyclic voltammetry under ambient conditions for the Pt|$SrTiO_{3-\delta}$|Pt bits, Figure 1d. We measured the hysteretic and bipolar[6] *I–V* profiles at constant voltage sweep rates of 50 mV s^{-1} and maximum bias of ±4 V per bit. During the positive voltage sweep the conductivity increased and switched the resistance of the device to a lowered value; in other words the switch was set to the "ON" state for voltages > +2.5 V. By cycling to negative voltages the conductivity decreased again and the Pt|$SrTiO_{3-\delta}$|Pt bit switched back to its high resistance state; the switch was set to its "OFF" state at voltages < –1.8 V. We obtained a resistance ratio of up to 43 for the hysteresis at +3 V. The corresponding critical electrical field strength of 3.5×10^6 V m^{-1} is in agreement with earlier reports for the $SrTiO_{3-\delta}$ anionic–electronic resistive switching material.[11–18] The hysteretic *I–V* profiles for a bias of ±4 V showed an asymmetry that is typical for bipolar anionic–electronic switches;[54] that is the absolute measured value of I_{SET}, defined by the maximum positive current, is up to two orders of magnitudes larger than the absolute value of I_{RESET}, defined by the highest negative current. The general mechanism discussed in the literature explains the observed resistive switching characteristics under ambient conditions through changes of the valence state of the titanium transition metal ion under the high electrical field. This leads to changes in the oxygen anionic and electronic defect concentration profiles and their mobilities upon a polarity change of the bias, see our earlier work for details.[18] We were able to demonstrate a stable and non-volatile resistive switching stability for more than 200 consecutive cycles, Figure 1d. It is interesting to note that the Pt|$SrTiO_{3-\delta}$|Pt resistive switching bits required no pre-forming steps as is usually the case for this type of material.[12] After 20 initial cycles during which the switching stabilized in its set and reset currents (I_{SET} and I_{RESET}), see Figure S2 in the Supporting Information, the structures can be operated with high reproducibility as demonstrated in Figure 1d. Furthermore, we repeated the experiment applying the same bias sweep conditions for five microelectrode sets, denoted as *E1* to *E5* in **Figure 2**a, confirming the high reproducibility of the bit-device structures processed for bipolar switches. For the capacitor-like structure of the sample the *I–V* profile is not pinned to the origin, but the zero-crossing of the current is clearly shifted by capacitive contributions. To obtain a better understanding of this capacitive behavior we carried out cyclic voltammetry measurements in the voltage window of –2 V to +2 V. The end voltages of these experiments are smaller than the switching threshold voltages for a constant sweep rate of 50 mV s^{-1}, see Figure 2b,c. The *I–V* profiles showed no non-volatile resistive switching, instead they showed a similar zero-crossing shift as was found for the voltage window of ±4 V. These *I–V* profiles correspond to the typical charging and discharging cyclic voltammetry curves of a capacitor with a parallel resistor. Based on this experimental evidence we deduced that the capacitive contributions are not linked to the resistive switching mechanism itself. The capacitive contributions fit well with our earlier reported chronoamperometry results and the suggested equivalent circuit models a memristor in parallel with a capacitor for such devices.[18]

We can conclude from these cycling voltammetry results in ambient atmosphere that we successfully fabricated Pt|$SrTiO_{3-\delta}$|Pt bits that exhibit bipolar resistive switching with memristive and capacitive contributions depending on the applied bias range. This basic electrical characterization of our devices demonstrates the good reproducibility and high uniformity. Stable resistive switching under ambient conditions enabled us to study the effect of humidity in the following experiments.

2.2. Impact of Humidity on Resistive Switching

To identify the influence of moisture on the resistive switching property, we examined the effect of relative humidity change on the cyclic voltammetry characteristics of the Pt|$SrTiO_{3-\delta}$|Pt

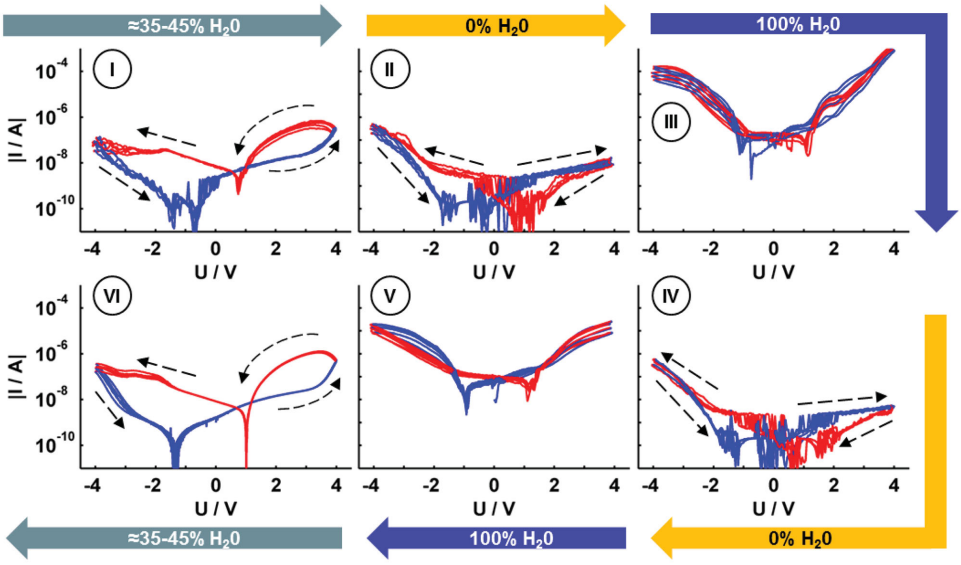

Figure 3. This figure shows five consecutive *I–V* profiles under three different humidity levels: i) Laboratory air with 35–45% relative humidity (atmosphere cycle I and VI). ii) Synthetic air with 0% relative humidity (atmosphere cycle II and IV). iii) Humidified synthetic air with 100% relative humidity (atmosphere cycle III and V). Blue lines show the increasing voltage branch and the red lines indicate the decreasing voltage branch. Depending on the humidity level the conductivity and the *I–V* profile shape changes drastically: in 0% humidity no resistive switching was observable. Comparison of cycles at the same humidity, for instance, humidity exposure cycles I and VI, shows that this process is fully reversible.

bits. The characteristic resistive switching cyclic voltammetry *I–V* profile varied systematically with the relative humidity and atmospheric humidity cycles applied (I–VI), see **Figure 3**. The following observations were made:

- The characteristic *I–V* hysteresis as measured in ambient air for a relative humidity around 40% is represented in cycle (I) of Figure 3. The *I–V* profile in this case was that of a non-volatile memory switch with counter-clock-wise switching and the characteristic resistance "ON" and "OFF" states are in agreement with the *I–V* profiles of Figure 1d.
- By exposing the switch to a dry atmosphere, both the shape of the *I–V* profile and the switching were strongly modified: we observed a change from the original anticlockwise switching to a capacitive hysteresis without crossover; in other words, the non-volatile memory characteristic vanished under dry air (0% relative humidity, atmosphere cycle II, Figure 3). The absolute conductivity decreased as is expected from theory because of the decreased protonic conduction of the oxides.[42]
- By increasing the relative humidity to 100% in atmosphere cycle III (Figure 3) the conductivity strongly increased and a third type of *I–V* profile shape was observed. In this case, nonlinear fluctuating currents were observed. Moreover, an *I–V* profile with multiple crossings was measured and no hysteresis behavior was observed.

We repeated the experiment involving the same relative atmospheric humidity changes and measured the Pt|$SrTiO_{3-\delta}$|Pt resistive switch response after consquently re-equilibration of at least 15 minutes to dry atmosphere, 100%, and 40% relative humidity exposure, see atmospheric cycles IV–VI in Figure 3. It can clearly be seen that the current–voltage profiles of the resistive switches show again the same switching directions, shapes, effective maximum current values, and R_{OFF}/R_{ON} ratios as in the atmosphereic cycles I–III. From this, we can conclude that the interactions of the $SrTiO_{3-\delta}$ thin film with moisture and synthetic versus laboratory air are fully reversible and the bit device structures are very robust. Excitingly, the resistive switch response can be fully tuned from a hysteretic current–voltage profile with addressable resistance states for relative humidity levels around 40% (Figure 3, atmosphere cycles I and VI) to a capacitive hysteresis without crossover (Figure 3, atmosphere cycles II and IV) or an almost non-hysteretic *I–V* profile with multiple crossings (Figure 3, atmosphere cycles III and V) in either completely dry or fully moisturized atmosphere. These results indicate that a certain amount of moisture or traces of gases that do not generally exist in synthetic air are required to achieve the anionic–electronic resistive switching in the metal-oxide films. The reversibility of the interaction of moisture with the memristance and the stable *I–V* profiles measured at 100% relative humidity show that a possible water-splitting reaction does not take place at the field strengths applied. In accordance to the literature[42] we observed a decrease in relative conductivity of the Pt|$SrTiO_{3-\delta}$|Pt resistive switch in the fully dry atmosphere, which increased under 100% relative humidity conditions. We have summarized the absolute switching currents I_{SET} and I_{RESET} for the six atmospheric cycles in **Figure 4**a,b. For I_{SET} at ambient conditions (atmosphere cycles I and VI) a value of 1.4×10^{-6} A was measured, which corresponds to a current density J of 5.6 A m^{-2}. Under dry conditions (atmosphere cycles II and IV) I_{SET} decreased by around 2 orders of magnitude to 5.5×10^{-8} A ($J = 0.22$ A m^{-2}), whereas for the 100% relative humidity a current as high as 3.2×10^{-4} A ($J = 1.3 \times 10^{3}$ A m^{-2}) was recorded. It can thus be concluded that I_{SET} of the resistive switch can vary impressively over 4 orders of magnitude depending on the humidity level at room temperature for the same electric

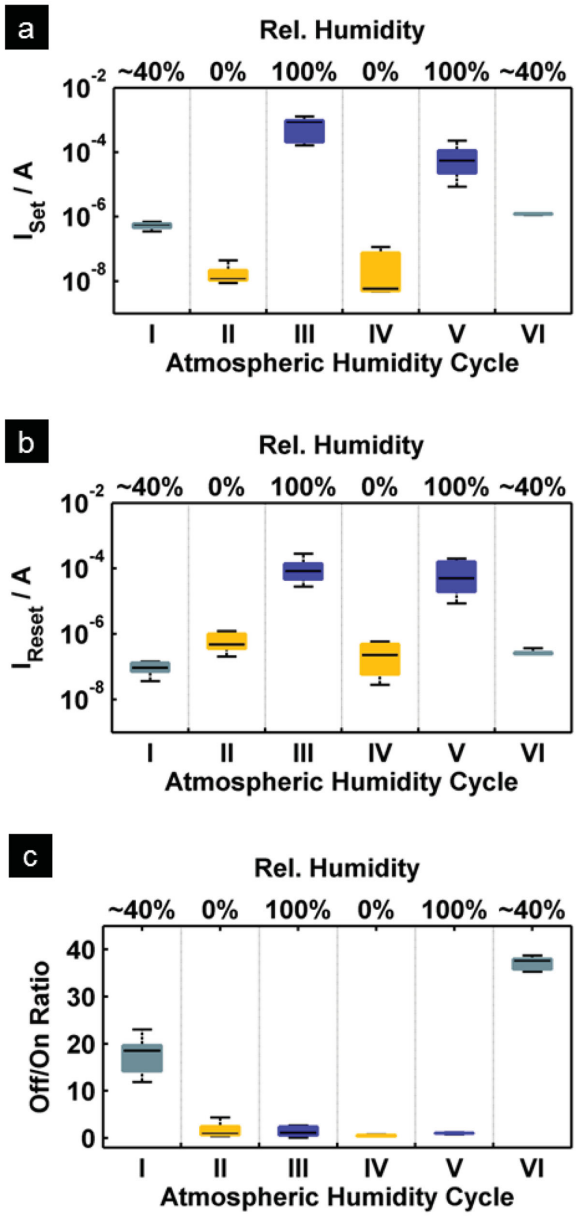

Figure 4. a) This figure shows I_{SET} referring to the maximum current at a single *I–V* profile for the six different measured atmosphere cycles. The higher the relative humidity, the higher the conductivity covering a range of four orders of magnitude. b) I_{RESET} refers to the highest negative current at a single *I–V* profile. c) Ratio of resistance states at +3 V for the different atmosphere cycles showing non-volatile resistive switching solely for intermediate relative humidity levels.

field strength of 5.5×10^6 V m^{-1}. In contrast I_{RESET} is much less sensitive to the humidity than I_{SET} and did not show such a significant difference between the ambient (-1.9×10^{-7} A) and dry conditions (-5.0×10^{-7} A). Only at 100% relative humidity a higher current of -9.3×10^{-5} A, which constituted a similarly large change as that for I_{SET}, was measured. This might arise from the fact that the conductivity at negative voltage is defined by the bottom electrode, which is not as exposed to the ambient humidity as the top electrode and therefore results in a lower sensitivity. The analysis of the resistance states at +3 V for the different atmosphere cycles shows that for 40% humidity a resistance ratio of up to 43 was measured and that for the 0% nor for the 100% relative humidity (ratio ca. 1) any resistive switching could be observed, see Figure 4c.

These results show that moisture indeed plays an important role in anionic–electronic memristive devices and thus also has to be taken into account in switching models. The interaction of moisture with oxide surfaces and the corresponding reaction mechanism and transport processes at high temperatures have been extensively studied,[33,47] and we have now unveiled the moisture interaction under ambient conditions and at room temperature. We can conclude that the incorporation of water molecules within the oxygen vacancies, the splitting of water molecules, as well as electronic processes play a crucial role. We have shown that the resistance switch characteristics, such as the memristance and its hysteresis current–voltage profile, can be fully transformed into predominantly capacitive characteristics by tuning the humidity.

Fundamentally, we can see that for these anionic–electronic resistive switches a similar response is obtained from the switches at moderate temperatures and under high electrical fields when exposed to humidity as compared to their behavior at high temperatures. It is reasonable to assume that moisture influences the overall electronic structure at the space-charge region of the metal|oxide interface, see schematic in **Figure 5**. Here a multi-step electrochemical reaction is involved: In the first step, the gas water molecule is adsorbed onto the Pt|$SrTiO_3$ resistive switch surface. Secondly, the adsorbed hydroxyl group interacts with the oxygen and anionic/electronic transfer occurs across the interface and at the space-charge region. Finally, a bulk oxygen anionic/electronic migration sets in, and depending on the degree of moisture a resistive switching response ranging from memristive (hysteretic current–voltage profile, 40% rel. humidity) to capacitive (0% rel. humidity) is obtained. Additional IR spectroscopy experiments revealed no evidence of OH groups in the $SrTiO_{3-\delta}$ bulk (OH-bands below detection limit). This further supports the fact that the water interaction is a surface-related process and affects the memristive response of the resistive switch. In conclusion, the electronic structure and Schottky barrier is altered by both the memristance itself and the interaction of moisture with the oxide, ultimately leading to the moisture interfering with the memristance itself of the oxide.

3. Conclusion

In this work, we have successfully fabricated Pt|$SrTiO_{3-\delta}$|Pt bits that show stable resistive switching characteristics over 200 cycles under ambient conditions. Using a model experiment we demonstrated for the first time that moisture has a strong impact on the resistive switching behavior of oxygen anionic–electronic switching metal-oxides, such as $SrTiO_3$, whereby this behavior is fully reversible. We show that the basic property of memristance is dependent on moisture, which is in line with earlier humidity sensing studies at lower electrical fields. At higher electrical fields the overall conductivity changes over about 4 orders of magnitude, and, moreover, the *I–V* profile

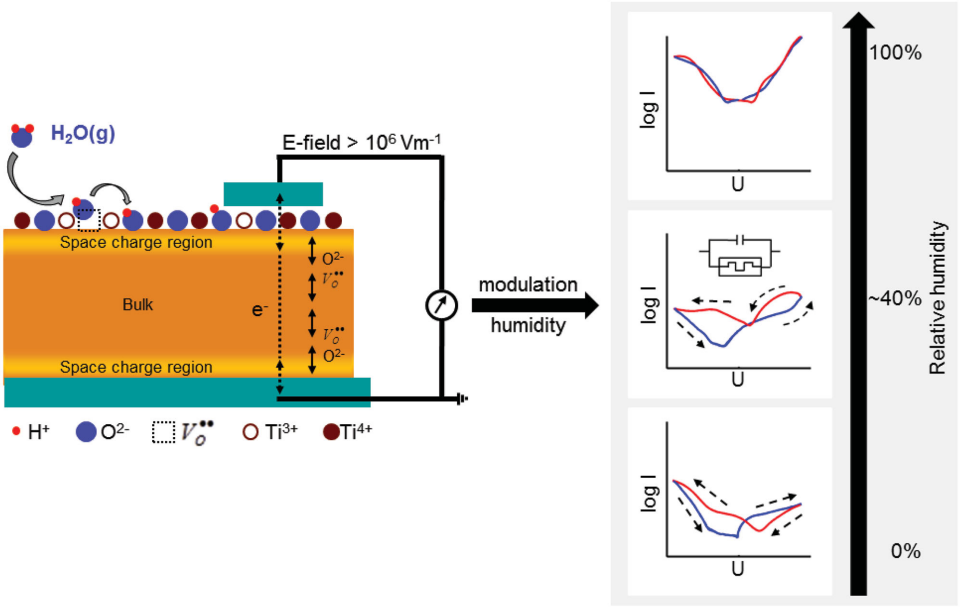

Figure 5. a) Schematic illustration of the interference of moisture with memristance. Water molecules are incorporated into the oxide through oxygen vacancies at the surface. The space-charge region and the Schottky barrier are modulated by this adsorption process and this interferes with the memristance itself. The *I–V* profiles change with moisture and vary from a capacitive-like behavior (0% rel. humidity) to memristive switching behavior (40% rel. humidity).

shape, number of crossings, and switching capability can be modified by tuning the ambient humidity.

In contrast to the measurable memristive behavior under ambient conditions, it was shown that in dry synthetic air only capacitive contributions and no resistive switching was obtained, which could be turned into a non-hysteretic *I–V* profile with multiple crossings by changing the relative humidity to 100%. This consequently has an enormous impact on the development of more precise switching models, material studies, as well as for final device geometries. First of all, today's switching models primarily do not consider the effect of moisture on the switching behavior, nor do they take into account the interaction between the surface species and hydroxyl groups present; they generally only focus on the anionic defects. Our experimental results, however, clearly demonstrate that moisture, resulting in the formation of hydroxyl groups at the surface of the oxide material, has to be taken into account when developing more precise switching models, materials, and their involved charge carriers. We considered the interaction of moisture with the Schottky barrier at the oxide interface as the most likely origin of the interference with the memristance. Also, the humidity level has to be controlled when carrying out material and/or device studies, for instance, for the doping of metal oxides, to obtain comparable results and to draw correct conclusions from electrical measurements for diffusion models under high electric fields for resistive switch development. Therefore, we suggest standard tracking of the humidity level for anionic–electronic resistive switching studies, similar to which is done for cationic switches.[48] It might become crucial to introduce a capping layer into all anionic–electronic resistive switching devices to maintain a constant moisture influence on the oxide and to avoid switching variations over time arising from changes in humidity during operation. Despite the recent advances in the field of oxygen anionic-based switches a breakthrough on the industrial scale has so far not been achieved yet, which may mainly be because of the lack of control over the uniformity and variability of these devices.[54,55] Discussions so far on this topic were mainly restricted to controlling the microstructure and surface roughness of the materials.[55,56] The impact of moisture on the uniformity and variability of metal-oxide ReRAM devices was so far hardly ever considered, although, as we have demonstrated, it plays a crucial role in the case of strontium titanate as the oxygen anionic–electronic resistive switching material.

From a fundamental perspective, these results show that moisture cannot be neglected in the development of anionic–electronic resistive switches as hydroxyl interactions seem to be crucial to the basic property of memristance. These new insights on the humidity controlling the current–voltage profile transition from a classic memristive behavior to a fully capacitive one allow us to formulate future device design guidelines to tweak the resistance ratios and their addressable states and to engineer high-performance anionic–electronic resistive switches.

4. Experimental Section

Sample Preparation and Characterization: The electrodes were structured via a standard photolithography process on round sapphire substrates. The micropatterning of the electrodes was carried out in a ISO class 4 cleanroom using AZ nLOF 2070 (1:0.4) negative photoresist (Microchemicals, Germany), which was spun at a speed of 4750 rpm for 45 s and softbaked at 110 °C for 180 s. The samples were then rehydrated for at least 10 minutes before alignment and exposure to ultraviolet light (210 mJ cm^{-2}) with a mask aligner (Karl-Zeiss MJ3B) using a custom made foil mask (Selba, Switzerland). Finally the structures were developed with MIF 726 developer for 90 s and rinsed in water. An O_2

plasma asher (Technics Plasma TePla 100 asher system) was employed for 60 s at 100 W to clean the surfaces of the samples of any organic residues before metal deposition. The bottom electrodes consisted of a titanium adhesion layer of 5 nm in thickness and an 80-nm thick platinum layer deposited via electron beam evaporation (Plassys MEB 550). The top electrodes with an area of 500 μm × 500 μm consisted of pure platinum and were deposited in the same manner. The 760-nm thick strontium titanate film was deposited via pulsed laser deposition (Surface Advanced PLD technology; KrF excimer laser, 248 nm) at a laser energy density of 0.6 J cm^{-2} per pulse and a deposition frequency of 10 Hz under a constant oxygen flow at a pressure of 0.0267 mbar at 700 °C. The thin-film layer thicknesses were confirmed by cross-view electron scanning images (LEO 530, Zeiss) and profilometer measurements (Dektak XT Advanced profilometer, Bruker). The sample fabrication process was described in detail in one of our previous reports.[18] All samples and PLD targets were characterized via X-ray diffraction (Bruker, D8, Cu Kα) and the cubic phase was confirmed, see Supporting Information Figure S1. For structural characterization the sample was cleaved after electrical characterization and a 5-nm thick platinum layer was sputtered onto it to record the cross-view scanning electron microscopy images (LEO 530, Zeiss) at an acceleration voltage of 3 kV.

Electrical Characterization: All electrical measurements were carried out with either a Keithley Source Meter Unit 2601b or a Keithley High Resistance Meter 6517b. The electrodes were brought into contact with platinum contact needles controlled by micro positioners and employing a stereo light microscope (Nikon SMZ 1500). The top electrodes were set as the working electrode and the bottom electrodes were grounded. To avoid complicated conduction path interpretations, so-called sneak paths,[57] all data shown in this study were measured on single Pt|$SrTiO_{3-\delta}$|Pt bits. If not otherwise noted the cyclic voltammetry experiments were carried out between ±4V at a constant sweep rate of 50 mVs^{-1} at room temperature. Before measurements were carried out the pristine electrodes were cycled at least 15 times to reach a stable switching state, no additional electroforming was necessary. To verify the reproducibility of our study at least three electrodes were measured each time and under the same conditions. The cyclic voltammetry measurements under different humidity levels were carried out in a custom-made, closed, high-vacuum microprobe station (Everbeeing Taiwan and Electrochemical Materials ETH Zurich Switzerland). For a relative humidity level of 35–45% the electrical measurements were carried out under ambient atmosphere. A dry atmosphere with 0% relative humidity was achieved by reducing the pressure in the microprobe station to 2×10^{-2} mbar and then flushing the chamber with synthetic air (20% O_2, 80% N_2, H_2O < 3 ppm). The evacuation and flushing step was repeated three times to ensure a dry atmosphere. The electrical measurements were carried under a constant gas flow of 1 sccm at ambient pressure. For the measurements with 100% relative humidity the synthetic air was passed through a gas-wash bottle filled with H_2O before entering the microprobe station.

Supporting Information

Supporting Information is available from the Wiley Online Library or from the author.

Acknowledgements

The authors thank S. Schweiger for support with the XRD measurements and Prof. R. Nesper and Dr. M. Wörle for the use of the XRD facility. Funding of this project by the Swiss National Science Foundation Projects 138914, 155986, 144988 is also gratefully acknowledged.

Received: April 15, 2015
Revised: May 16, 2015
Published online: July 14, 2015

[1] *International Technology Roadmap for Semiconductor Industry* (ITRS) 2011 Edition, Emerging Research Materials, http://www.itrs.net/, (accessed: December 2014).
[2] Y. V. Pershin, M. Di Ventra, *Adv. Phys.* **2011**, *60*, 145.
[3] T. W. Hickmott, *J. Appl. Phys.* **1962**, *33*, 2669.
[4] D. B. Strukov, G. S. Snider, D. R. Stewart, R. S. Williams, *Nature* **2009**, *453*, 80.
[5] L. O. Chua, *IEEE Trans. Circuits Systems* **1971**, *Ct18*, 507.
[6] R. Waser, R. Dittmann, G. Staikov, K. Szot, *Adv. Mater.* **2009**, *21*, 2632.
[7] Y. Watanabe, J. G. Bednorz, A. Bietsch, C. Gerber, D. Widmer, A. Beck, S. J. Wind, *Appl. Phys. Lett.* **2001**, *78*, 3738.
[8] R. Bruchhaus, R. Waser, in *Thin Film Metal-Oxides* (Ed: Shriram Ramanathan) Springer, **2010**, pp 131–167.
[9] F. Pan, S. Gao, C. Chen, C. Song, F. Zeng, *Mater. Sci. Eng.: Reports* **2014**, *83*, 1.
[10] D. J. Seong, M. Jo, D. Lee, H. Hwang, *Electrochem. Solid State Lett.* **2007**, *10*, H168.
[11] D. Panda, T. Y. Tseng, *Ferroelectrics* **2014**, *471*, 23.
[12] X. Guo, *Appl. Phys. Lett.* **2012**, *101*, 152903.
[13] S. Menzel, M. Waters, A. Marchewka, U. Bottger, R. Dittmann, R. Waser, *Adv. Funct. Mater.* **2011**, *21*, 4487.
[14] X. W. Sun, G. Q. Li, L. Chen, Z. H. Shi, W. F. Zhang, *Nanoscale Res. Lett.* **2011**, *6*, 599.
[15] R. Oligschlaeger, R. Waser, R. Meyer, S. Karthauser, R. Dittmann, *Appl. Phys. Lett.* **2006**, *88*, 042901.
[16] C. Park, Y. Seo, J. Jung, D.-W. Kim, *J. Appl. Phys.* **2008**, *103*, 054106.
[17] S. Saraf, M. Markovich, T. Vincent, R. Rechter, A. Rothschild, *Appl. Phys. Lett.* **2013**, *102*, 022902.
[18] F. Messerschmitt, M. Kubicek, S. Schweiger, J. L. M. Rupp, *Adv. Funct. Mater.* **2014**, *24*, 7448.
[19] R. A. Cowley, *Phil. Trans. R. Soc. Lond. A* **1996**, *354*, 2799.
[20] R. Perez-Casero, J. Perrière, A. Gutierrez-Llorente, D. Defourneau, E. Millon, W. Seiler, L. Soriano, *Phys. Rev. B* **2007**, *75*, 165–317.
[21] R. Merkle, J. Maier, *Angew. Chem. Int. Ed.* **2008**, *47*, 3874.
[22] U. Balachandran, N. G. Eror, *J. Solid State Chem.* **1981**, *39*, 351.
[23] V. Metlenko, A. H. Ramadan, F. Gunkel, H. Du, H. Schraknepper, S. Hoffmann-Eifert, R. Dittmann, R. Waser, R. A. De Souza, *Nanoscale* **2014**, *6*, 12864.
[24] D. Marrocchelli, L. Sun, B. Yildiz, *J. Am. Ceram. Soc.* **2015**, *137*, 4735.
[25] R. Muenstermann, T. Menke, R. Dittmann, R. Waser, *Adv. Mater.* **2010**, *22*, 4819.
[26] A. Sawa, *Mater. Today* **2008**, *11*, 28.
[27] H. Akinaga, H. Shima, *Proc. IEEE* **2010**, *98*, 2237.
[28] T. Menke, R. Dittmann, P. Meuffels, K. Szot, R. Waser, *J. Appl. Phys.* **2009**, *106*, 114507.
[29] K. Szot, W. Speier, G. Bihlmayer, R. Waser, *Nat. Mater.* **2006**, *5*, 312.
[30] J. W. Mares, J. S. Fain, S. M. Weiss, *Phys. Rev. B* **2013**, *88*, 075307.
[31] M. Wojtyniak, K. Szot, R. Wrzalik, C. Rodenbücher, G. Roth, R. Waser, *J. Appl. Phys.* **2013**, *113*, 083713.
[32] T. Seiyama, N. Yamazoe, H. Arai, *Sensors Actuators* **1983**, *4*, 85.
[33] Z. A. Feng, F. El Gabaly, X. Ye, Z. X. Shen, W. C. Chueh, *Nat. Commun.* **2014**, *5*, 4374.
[34] M. Shirpour, G. Gregori, R. Merkle, J. Maier, *Phys. Chem. Chem. Phys.* **2011**, *13*, 937.
[35] N. Barsan, U. Weimar, *J. Electroceramics* **2001**, *7*, 143.
[36] I. Riess, S. Raz, K. Sasaki, J. Maier, *Proc. Electrochem. Soc.* **2001**, *28*, 267.
[37] S. M. Ke, H. T. Huang, H. Q. Fan, H. L. W. Chan, L. M. Zhou, *Solid State Ionics* **2008**, *179*, 1632.
[38] S. Agarwal, G. L. Sharma, R. Manchanda, *Solid State Commun.* **2001**, *119*, 681.
[39] Z. Chen, C. Lu, *Sensors Lett.* **2005**, *3*, 274.

[40] S. Steinsvik, Y. Larring, T. Norby, *Solid State Ionics* **2001**, *143*, 103.
[41] R. Waser, *Ber. Bunsenges. Phys. Chem.* **1986**, *90*, 1223.
[42] W. Qu, R. Green, M. Austin, *Meas. Sci. Technol.* **2000**, *11*, 1111.
[43] Y. Yamazaki, P. Babilo, S. M. Haile, *Chem. Mater.* **2008**, *20*, 6352.
[44] R. B. Cervera, Y. Oyama, S. Miyoshi, I. Oikawa, H. Takamura, S. Yamaguchi, *Solid State Ionics* **2014**, *264*, 1.
[45] Q. Chen, F. El Gabaly, F. Aksoy Akgul, Z. Liu, B. S. Mun, S. Yamaguchi, A. Braun, *Chem. Mater.* **2013**, *25*, 4690.
[46] E. Fabbri, L. Bi, D. Pergolesi, E. Traversa, *Adv. Mater.* **2012**, *24*, 195.
[47] K. D. Kreuer, *Annu. Rev. Mater. Res.* **2003**, *33*, 333.
[48] S. Tappertzhofen, I. Valov, T. Tsuruoka, T. Hasegawa, R. Waser, M. Aono, *ACS Nano* **2013**, *7*, 6396.
[49] T. Tsuruoka, K. Terabe, T. Hasegawa, I. Valov, R. Waser, M. Aono, *Adv. Funct. Mater.* **2012**, *22*, 70.
[50] F. Aguesse, A. K. Axelsson, P. Reinhard, V. Tileli, J. L. M. Rupp, N. M. Alford, *Thin Solid Films* **2013**, *539*, 384.
[51] E. J. Tarsa, E. A. Hachfeld, F. T. Quinlan, J. S. Speck, M. Eddy, *Appl. Phys. Lett.* **1996**, *68*, 490.
[52] Y. Chen, W. Jung, Z. Cai, J. J. Kim, H. L. Tuller, B. Yildiz, *En. Environ. Sci.* **2012**, *5*, 7979.
[53] Y. A. Abramov, V. G. Tsirelson, V. E. Zavodnik, S. A. Ivanov, I. D. Brown, *Acta Crystallogr. B* **1995**, *51*, 942.
[54] S. Menzel, R. Waser, *Phys. Status Solidi – Rapid Res. Lett.* **2014**, *8*, 540.
[55] N. Raghavan, *Microelectron. Reliab.* **2014**, *54*, 2253.
[56] N. Raghavan, M. Bosman, D. D. Frey, K. L. Pey, *Microelectron. Reliab.* **2014**, *54*, 2266.
[57] E. Linn, R. Rosezin, C. Kugeler, R. Waser, *Nat. Mater.* **2010**, *9*, 403.